Glycoconj J
DOI 10.1007/s10719-016-9722-y

ORIGINAL ARTICLE

A novel biological function of soluble biglycan: Induction of erythropoietin production and polycythemia

Helena Frey[1] · Kristin Moreth[2] · Louise Tzung-Harn Hsieh[1] · Jinyang Zeng-Brouwers[1] · Birgit Rathkolb[2,3] · Helmut Fuchs[2] · Valérie Gailus-Durner[2] · Renato V. Iozzo[4] · Martin Hrabě de Angelis[2,5,6] · Liliana Schaefer[1]

Received: 31 May 2016 / Revised: 4 August 2016 / Accepted: 5 August 2016

Abstract Secondary polycythemia, a disease characterized by a selective increase in circulating mature erythrocytes, is caused by enhanced erythropoietin (Epo) concentrations triggered by hypoxia-inducible factor-2α (HIF-2α). While mechanisms of hypoxia-dependent stabilization of HIF-2α protein are well established, data regarding oxygen-independent regulation of HIF-2α are sparse. In this study, we generated a novel transgenic mouse model, in which biglycan was constitutively overexpressed and secreted by hepatocytes (BGN^{Tg}), thereby providing a constant source of biglycan released into the blood stream. We discovered that although the mice were apparently normal, they harbored an increase in mature circulating erythrocytes. In addition to erythrocytosis, the BGN^{Tg} mice showed elevated hemoglobin concentrations, hematocrit values and enhanced total iron binding capacity, revealing a clinical picture of polycythemia. In BGN^{Tg} mice markedly enhanced *Epo* mRNA expression was observed in the liver and kidney, while elevated Epo protein levels were found in liver, kidney and blood. Mechanistically, we showed that the transgenic animals had an abundance of HIF-2α protein in the liver and kidney. Finally, by transiently overexpressing circulating biglycan in mice deficient in various Toll-like receptors (TLRs), we determined that this novel function of biglycan to promote Epo synthesis was specifically mediated by a selective interaction with TLR2. Thus, we discovered a novel biological pathway of soluble biglycan inducing HIF-2α protein stabilization and Epo production presumably in an oxygen-independent manner, ultimately giving rise to secondary polycythemia.

Keywords Proteoglycan · Extracellular matrix · Erythrocyte · Hypoxia-inducible factor · Toll-like receptor · Damage-associated molecular pattern

Helena Frey and Kristin Moreth contributed equally to this work.

✉ Liliana Schaefer
schaefer@med.uni-frankfurt.de

1 Pharmazentrum Frankfurt, Institut für Allgemeine Pharmakologie und Toxikologie, Klinikum der Goethe-Universität Frankfurt am Main, Frankfurt am Main, Germany

2 German Center for Environmental Health, Institute of Experimental Genetics and the German Mouse Clinic, Helmholtz-Zentrum München, Neuherberg, Germany

3 Gene Center, Institute of Molecular Animal Breeding and Biotechnology, Ludwig-Maximilians-Universität München, Feodor-Lynen Strasse 25, 81377 Munich, Germany

4 Department of Pathology, Anatomy and Cell Biology, Sidney Kimmel Medical College at Thomas Jefferson University, Philadelphia, PA 19107, USA

5 Lehrstuhl für Experimentelle Genetik, Center of Life and Food Science, Weihenstephan Technische Universität München, Freising-Weihenstephan, Germany

6 German Center for Diabetes Research, Neuherberg, Germany

Abbreviations

Bgn	Biglycan
ECM	Extracellular matrix
Epo	Erythropoietin
HIF	Hypoxia-inducible factor
NF-κB	Nuclear factor kappa-light chain enhancer of activated B-cells
NO	Nitric oxide
PAS	Periodic acid–Schiff
PHD	Prolyl hydroxylase
ROS	Reactive oxygen species
RP	Red pulp
TIBC	Total iron binding capacity

TLR	Toll-like receptor
VHL	Von Hippel-Lindau protein
WP	White pulp

Introduction

Polycythemia is a disease characterized by an increased number of mature erythrocytes in the circulation causing enhanced blood viscosity and thereby augmenting the clinical risk of thrombosis, cardiac infarction and stroke [1, 2]. Primary polycythemia (*polycythemia rubra vera* or Vaquez' disease) is a chronic myeloproliferative disorder of the bone marrow marked by enhanced number of erythrocytes, leukocytes and thrombocytes and low levels of erythropoietin (Epo). In contrast, secondary polycythemia, frequently induced by hypoxic conditions such as heavy smoking, chronic obstructive pulmonary diseases and living at high altitude, is caused by enhanced Epo concentrations with selective increase of the erythrocyte number [3]. Epo, a protein of 30 kDa, is in adults mainly produced in the kidney by interstitial cells and to some degree in the liver by hepatocytes [4–6]. Epo is a crucial regulator of erythropoiesis that stimulates the proliferation and terminal differentiation of erythroid precursor cells [4, 7]. Therefore, administration of recombinant Epo has become the standard treatment for anemia in chronic kidney disease [8].

The transcription of the *Epo* gene is tightly regulated by various oxygen-sensing mechanisms [8, 9]. A key hypoxia-inducible transcription factor that regulates Epo production is the so-called Endothelial PAS domain-containing protein 1 (EPAS1), also known as hypoxia-inducible factor-2α (HIF-2α) [10]. Mutations in *EPAS1* genes cause erythrocytosis familial type 4 [11] and are associated with pulmonary hypertension and chronic mountain sickness [12]. Under physiological (non-hypoxic) conditions, HIF-2α is unstable due to hydroxylation of its α-subunit by prolyl hydroxylase domain proteins (PHDs), resulting in ubiquitination and degradation [10]. By contrast, upon hypoxia PHD-mediated posttranslational modification of HIF-2α is inhibited, leading to its stabilization and subsequent transcription of HIF-2α target genes [13]. Besides hypoxia, nitric oxide (NO), reactive oxygen species (ROS), succinate, fumarate, cobalt chloride and iron chelators have been shown to protect HIF-2α from degradation, resulting in increased Epo expression [8, 14]. In turn, several growth factors, tumor suppressors and oncogenes have been shown to stabilize HIF-1α [15]. Taken account that HIF-2α is crucial in Epo production, it is surprising that data regarding oxygen-independent regulation of HIF-2α are rather sparse.

There is growing evidence that components of the extracellular matrix (ECM) have not only a structural function within the ECM but may also act in their soluble form as signaling molecules [16, 17]. Biglycan, a class I small leucine-rich proteoglycan [16], is proteolytically released from the ECM upon tissue stress or injury as a soluble molecule thereby acting as a danger signal [18–21]. As an endogenous ligand of the innate immune receptors such as Toll-like receptor (TLR)-2 and -4 [20–23], soluble biglycan promotes inflammation via its ability to evoke the expression of pro-inflammatory cytokines and chemokines [22, 24–26]. We have previously established that transient overexpression of soluble biglycan in mice exerts profound pro-inflammatory effects and provided a direct *in vivo* proof for biglycan signaling via TLR2/4 [25–27]. Moreover, we have shown in the same mouse model that soluble biglycan can differentially target either one of the TLRs or its associated adaptor molecules, thereby regulating the inflammatory response and disease outcome [26–28]. It is now well accepted that circulating biglycan levels correlate with organ dysfunction in sterile and pathogen-induced inflammation [19]. However, the *in vivo* consequences of a chronic exposure to soluble biglycan have not been investigated yet.

In this study, we generated a mouse line stably overexpressing soluble human biglycan (BGN^{Tg}). Surprisingly, BGN^{Tg} mice exhibited markedly enhanced Epo levels that were associated with higher HIF-2α levels and increased erythrocyte numbers. We found that this novel biological activity of biglycan to induce Epo synthesis required exclusively TLR2. To the best of our knowledge, this is the first report of a soluble proteoglycan stimulating Epo synthesis and red blood cell production *in vivo* by enhancing HIF-2α levels in the liver and kidney.

Materials and methods

Animal experiments

C57BL/6J mice (referred to as "WT") were purchased from Jackson Laboratories (Bar Harbor, ME). $Tlr2^{-/-}$ and $Tlr4^{-/-}$ mice were generously provided by Dr. M. Freudenberg (Max Planck Institute for Immunology, Freiburg, Germany). $Tlr2^{-/-}$*/4-m* mice ($Tlr2^{-/-}$ mice carrying a functional TLR4 mutation) were generously provided by Prof. C. Kirschning (Technical University of Munich, Munich, Germany) [29, 30]. To overexpress biglycan in liver, the 1.1-kb full-length cDNA fragment of human biglycan was inserted downstream of the *Xho*I/*Xba*I site of pGEMAlbSVPA vector containing the albumin enhancer-promoter (E/P) sequence. The 4.7 kb biglycan transgene construct was linearized by *Apa*I/*Pvu*II and purified. The h*BGN* transgenic founders (BGN^{Tg}) were generated by microinjection of the linearized DNA into C57BL/6J zygotes. Potential founders were identified by genotyping PCR. Total genomic DNA was isolated from tail biopsies by KAPA Mouse Genotyping Hot Start Kit (PEQLAB, Germany) and subjected to PCR with primers binding within the albumin E/P sequence and h*BGN* cDNA sequence, yielding a band of 410 bp. The following primer

pair was used: 5′-CTG CAC ACA CGA TCA CCT TT-3′ and 5′-TTG TTG TTC ACC AGG ACG AG-3′. The *BGN*^{Tg} founders were then backcrossed to C57BL/6J mice for more than 30 generations to evaluate breeding potential and transgene transmissibility. No special feeding or breeding procedures have been used. 8–12 weeks old male mice were used for experiments. All animal work was conducted in accordance with the German Animal Protection Law and was approved by the Ethics Review Committee for Laboratory Animals of the District Government of Darmstadt, Germany.

Hematological screening

Thirty WT and *BGN*^{Tg} mice, with 15 male and 15 female each, all born within 1 week, were shipped to the German Mouse Clinic (GMC) for hematological analysis. At the GMC, mice were kept in IVC cages with water and standard mouse chow (Altromin no. 1314) according to the GMC housing conditions and German laws. Blood samples were collected from isoflurane-anesthetized mice by retro-bulbar puncture using a glass capillary (0.8 mm outer diameter). About 50 µl was collected in an EDTA-coated end-to-end capillary and diluted 1:5 with cell pack buffer (Sysmex Capillary tube, Sysmex Deutschland, Norderstedt, Germany) for hematological analysis. An additional aliquot of blood was collected in a Li-heparin coated sample tube (Kabe Labortechnik, Nümbrecht-Elsenroth, Germany) for clinical chemistry measurements. Diluted EDTA blood samples were analyzed using a Sysmex XT200iV blood cell counter to determine erythrocyte count, hemoglobin concentration as well as calculated hematocrit [31]. Heparin-blood samples were stored at room temperature for up to 2 h before being separated by centrifugation with 5000 x g for 10 min at 8 °C (Biofuge fresco, Heraeus, Germany). Plasma was transferred to 1.5 ml Eppendorf tubes, diluted 1:2 with deionized water and analyzed for a standard set of 20 clinical chemistry parameters including iron and unsaturated iron binding capacity by applying test kits provided by Beckman-Coulter using an AU480 auto-analyzer (Beckman-Coulter Germany, Krefeld, Germany) as described previously [32]. Total iron binding capacity was calculated as the sum of iron concentration and unsaturated iron binding capacity. All tests performed at the GMC were approved by the responsible authority of the Government of Upper Bavaria, Germany. For erythrocyte count from mice transiently overexpressing biglycan, 50 µl of heparinized blood was diluted 1:10,000 in PBS and erythrocytes counted in a counting chamber under the microscope. The counting was performed by 2 independent scientists blinded to the conditions.

Real-time quantitative polymerase chain reaction

Total RNA was extracted from kidneys and liver using the TRIreagent (Sigma Aldrich, Heidelberg, Germany) as described [33]. cDNA was reverse transcribed using the High Capacity cDNA Reverse Transcription Kit (Applied Biosystems, Germany). Real-time quantitative PCR was performed using AbiPrism 7500 Sequence Detection System and Luminaris High Green Low ROX qPCR Mastermix (Thermo Fisher Scientific, Germany) with the following primer pairs: human/mouse *BGN*, 5′-CTA CAT CTC CAA GAA CCA CCT G-3′ and 5′-ATG CAG TTC ATG TTC CGG AG-3′; mouse *Epo*, 5′-CTC AGA AGG AAT TGA TGT CG-3′ and 5′-AGT TGG CGT AGA CCC GGA AG-3′ and mouse *Gapdh*, 5′-CAT GGC CTT CCG TGT TCC TA-3′ and 5′-CCT GCT TCA CCA CCT TCT TGA T-3′. Relative changes in gene expression compared to control and normalized to *Gapdh* were quantified by the $2^{-\Delta\Delta Ct}$ method. For semi-quantitative RT-PCR the 5× Mastermix "ready to use" (Bio&Sell, Feucht, Germany) and the following primer pair were used: murine *Bgn*, 5′-AAC AAC CCT GTG CCC TAC TG-3′ and 5′-GCT TAG GAG TCA GGG GGA AG-3′; amplifying a band of 222 bp and human/murine *BGN*, 5′-TGG AGA ACA GTG GCT TTG AA-3′ and 5′-TGT TGA AGA GGC TGA TGC-3′, yielding a band of 428 bp. Only the product from h*BGN* transgene can be digested by *Sac*I to 268 and 160 bp.

Isolation and semi-quantification of biglycan from tissues and plasma

Biglycan from the kidney and liver homogenates as well as plasma samples (n = 3 for each group) was extracted and semi-purified as described previously [25, 33]. The glycosaminoglycan chains of the proteoglycan were then digested with chondroitinase ABC (Seikagaku Corporation, Tokyo, Japan) and the protein was subjected to polyacrylamide gel electrophoresis followed by Western blot analysis with subsequent quantification as described previously [25, 33]. A known amount of intact biglycan (containing protein core and glycosaminoglycan chains) was used as positive control for validation [33]. Purification and digestion with chondroitinase ABC of all samples was performed in parallel and under the same conditions. Renal and hepatic biglycan content was calculated per mg protein of organ homogenates used for proteoglycan isolation. Approximately 150 mg of kidney and liver and 200 µl of plasma were used for the isolation. The results of three isolations per group were averaged.

Western blot and ELISA

Epo protein concentration in organ lysates and plasma was measured by a mouse specific ELISA (BioLegend, London, UK) according to the manufacturer's instructions. For Western blot analysis, kidney and liver samples were homogenized and sonicated in lysis buffer containing 137 mM NaCl, 20 mM Tris/HCl, pH 8.0, 5 mM EDTA, 10 % glycerol, 1 % Triton X-100, centrifuged at 4 °C at 13,000 rpm for 15 min and

supernatants were snap-frozen and stored at −80 °C. Western blots were performed and quantified as described [33] using the following primary antibodies: goat anti-biglycan (TA302434, Acris Antibodies), mouse anti-β-Actin (A5441, Sigma Aldrich) and rabbit anti-mouse HIF-2α (NB100–122, Novus Biologicals). Secondary antibodies were rabbit anti-goat (H + L, Jackson ImmunoResearch), HRP-coupled donkey anti-rabbit (NA934V, GE Healthcare) and HRP-coupled sheep anti-mouse (NA931V, GE Healthcare). Signal detection was performed using the ECL Western blotting detection system (GE Healthcare, Freiburg, Germany) and optical density of bands was obtained using Scion Image Software (Scion Corporation).

Histopathology

For visualizing general structure of the tissue, periodic acid–Schiff (PAS) staining was performed. Sections (4 μm) of paraffin-embedded spleens from mice were deparaffinized and immersed in periodic acid solution (Applichem, Germany) for 10 min and further in Schiff's solution (Carl Roth, Germany) for 20 min after proper wash. Counterstaining was performed with Mayer's Hematoxylin (Sigma Aldrich, Germany). Quantification of red pulp (RP) and white pulp (WP) surface area was carried out using Scion Image Software. RP and WP surface area was measured across the entire surface area of the central longitudinal spleen section, the RP/WP ratio and the percentage of RP was then calculated.

For Perls' Prussian blue staining, deparaffinized tissue sections were immersed in the mixed solution of 10 % potassium ferrocyanide (Applichem, Germany) and 20 % hydrochloric acid (Sigma Aldrich, Germany) for 20 min. Counterstaining was proceeded with Nuclear fast red (Sigma Aldrich, Germany). At least 10 high-power fields (magnification, ×10) per section for each sample were examined. Perls' Prussian blue staining was quantified by determination of chromogen intensity using software ImageJ-Fiji version. Histological examinations were performed by 2 pathologists blinded to the conditions.

Transient overexpression of soluble biglycan *in vivo*

To generate mice transiently overexpressing soluble biglycan, human biglycan cDNA (h*BGN*) was inserted into the *BamHI*/*Sac*II site of the pLIVE™ (Liver *In Vivo* Expression) vector containing the mouse albumin promoter (Mirus Bio, Madison, USA) [26, 27]. Human biglycan was expressed in male mice by a single intravenous injection of the h*BGN* pLIVE vector (50 μg) in 400 μl of 5 % glucose and 6 μl of TurboFect *In Vivo* Transfection Reagent (Thermo Fisher Scientific, Schwerte, Germany) under 2 % isofluorane (Abbott laboratories, Wiesbaden, Germany) and 1 l/min oxygen anesthesia. For controls, empty pLIVE vector was used (pLIVE). Mice were sacrificed for collection of blood and organs 3-days after injection.

Statistics

All data are expressed as means ± S.D. Two-sided Student's *t* test was used to evaluate significance of differences between groups. Differences were considered significant with $P < 0.05$. Note that *P*-values are not corrected for multiple testing. In box plots single values are presented with 10th and 90th percentile whiskers. Each data point outside the 10th and 90th percentiles is plotted.

Results

Generation of mice stably overexpressing soluble biglycan

To address the clinical consequences of chronically-enhanced plasma levels of soluble biglycan, we generated a mouse line stably overexpressing human biglycan (BGN^{Tg}) exclusively in the liver. Analogous to our mouse model of transient overexpression of soluble biglycan [25, 27], we expected that hepatocytes would release this proteoglycan into the circulation where it would target various organs via ligand-receptor interactions. To this end, we cloned the full-length human biglycan cDNA downstream of the albumin promoter (Fig. 1a) to ensure organ-specific and continuous overexpression of the transgene by hepatocytes. The construct was then introduced into fertilized pronuclei of C57BL/6J mice where it was inserted into the genomic DNA by homologous recombination. The resulting mice overexpressing human biglycan were identified by genotyping (Fig. 1b) and crossed to obtain homozygosity. qRT-PCR with primers detecting both murine and human biglycan verified an 18-fold increase in *biglycan* mRNA expression in liver of BGN^{Tg} mice compared to age-matched (8 weeks-old) wild-type (WT) littermates (Fig. 1c). Semi-quantitative RT-PCR with primers specific for murine biglycan demonstrated no difference in the expression of endogenous biglycan in the liver of WT and BGN^{Tg} mice (Fig. 1d). cDNA isolated from human embryonic kidney (HEK) cells stably overexpressing human biglycan was used as negative control to verify the specificity. Human and murine biglycan genes share a 90 % homology; however, benefiting from an additional *Sac*I restriction site on human biglycan cDNA, we designed a PCR to distinguish the transgene from the endogenous transcriptions. With *Sac*I digestion, we confirmed that the increase in *biglycan* mRNA expression (Fig. 1c) was due to the overexpression of the human transgene whereas the endogenous mRNA remained unchanged (Fig. 1e). Elevated *biglycan* mRNA expression resulted in a 3-fold increase of biglycan protein in the liver (WT 0.54 ± 0.30 vs. BGN^{Tg} 1.48 ± 0.24; $n = 3$; $P < 0.05$) (Fig. 1f) and a 2-fold increase in plasma (WT 0.14 ± 0.04 μg/ml vs. BGN^{Tg} 0.29 ± 0.10 μg/ml; $n = 3$; $P < 0.05$) (Fig. 1g). This was followed by enhanced

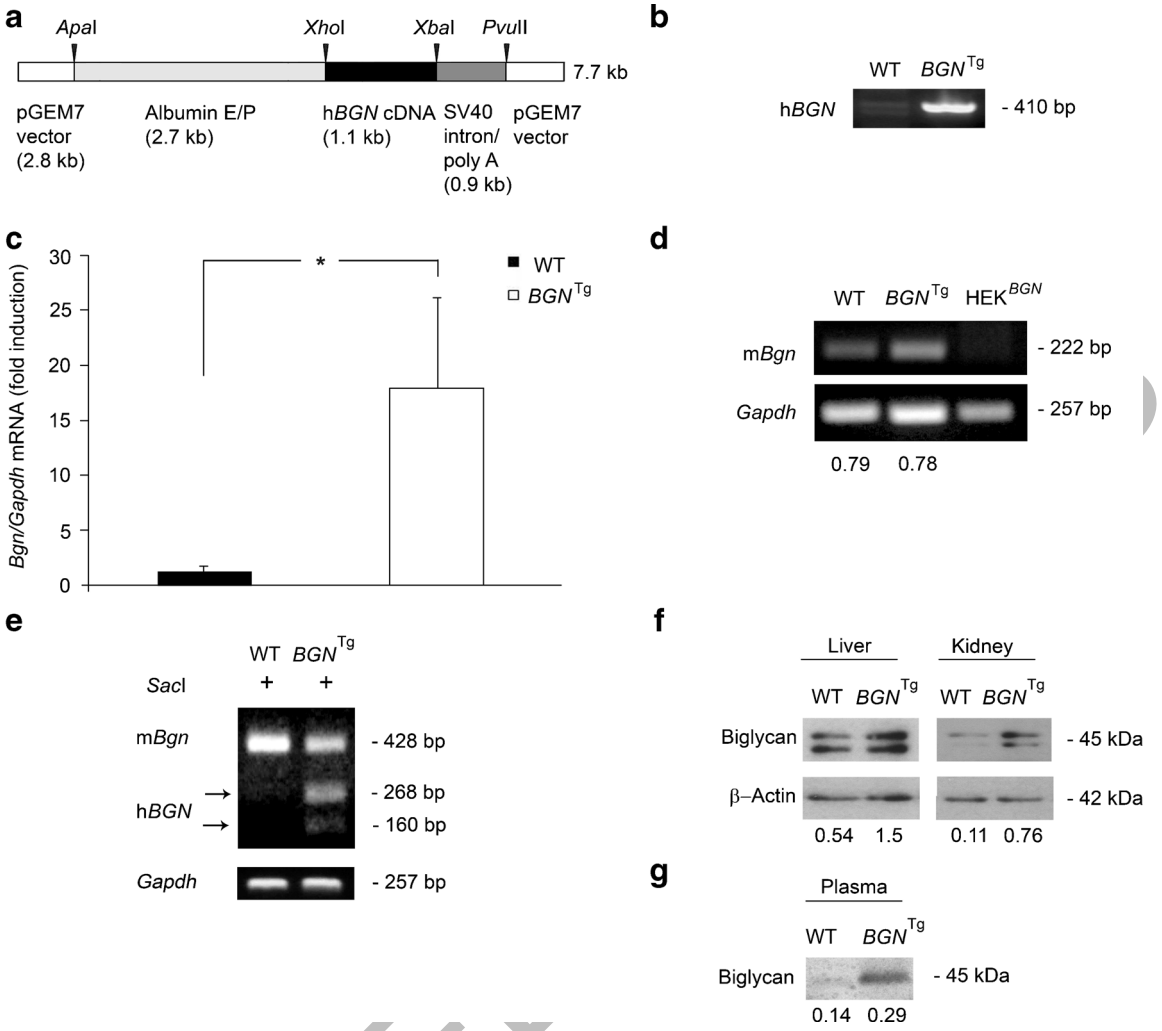

Fig. 1 Characterization of mice stably overexpressing soluble biglycan. (**a**) Linearized construct for overexpressing h*BGN* in hepatocytes, containing the full-length human biglycan cDNA after the albumin enhancer-promoter sequence (E/P). (**b**) Genotyping PCR analysis of wild-type (WT) and biglycan-overexpressing (BGN^{Tg}) mice. (**c**) Quantitative RT-PCR for human and murine *biglycan* mRNA expression in the liver of WT and BGN^{Tg} mice. mRNA expression was normalized to *Gapdh* and given as fold compared to WT mice; $n = 6$. Data represent means ± S.D.; asterisks indicate statistical significance with $^*P < 0.05$. (**d**) Semi-quantitative PCR of murine *biglycan* and *Gapdh* mRNA expression in the liver of WT and BGN^{Tg} mice; cDNA from human embryonic kidney cells stably overexpressing human biglycan (HEK^{BGN}) was used as a control. (**e**) PCR of human and murine *biglycan* mRNA expression in the liver of WT and BGN^{Tg} mice following *Sac*I digestion. Western blot analysis of biglycan protein core in the (**f**) liver, kidneys and (**g**) plasma as indicated. The numbers below the immunoblots represent the values normalized to β-Actin levels from 3 independent experiments

accumulation of biglycan protein in various organs, here shown for the kidney (WT 0.11 ± 0.04 vs. BGN^{Tg} 0.76 ± 0.38; $n = 3$; $P < 0.05$) (Fig. 1f). Similar results were obtained in 8–12 weeks-old mice. Thus, these data demonstrate an overexpression of human biglycan in the liver, followed by elevated levels of circulating biglycan with subsequent enhanced renal accumulation of this proteoglycan.

BGN^{Tg} mice develop polycythemia

BGN^{Tg} mice displayed no obvious phenotype, as the mice had normal growth, weight, lifespan and fertility. However, a hematological screening revealed higher erythrocyte count in BGN^{Tg} mice compared to their WT littermates (Fig. 2a). In contrast, no significant difference was observed in white blood cell count (WT 9.9 ± 3.0 × 10^3/mm^3 vs. BGN^{Tg} 12 ± 3.8 × 10^3/mm^3; $n = 15$; n.s.) and platelet count (WT 945 ± 202 × 10^3/mm^3 vs. BGN^{Tg} 1049 ± 155 × 10^3/mm^3; $n = 15$; n.s.). Complementing the increased erythrocyte number, BGN^{Tg} mice also revealed elevated hematocrit value (Fig. 2b) and enhanced hemoglobin concentrations (Fig. 2c). Analysis of the blood revealed no alteration in iron concentration (WT 19.7 ± 2.3 µmol/l vs. BGN^{Tg} 21.2 ± 2.3 µmol/l; $n = 15$; n.s.) or transferrin saturation (WT 32.8 ± 3.3 % vs. BGN^{Tg} 32.8 ± 3.2 %; $n = 15$; n.s.). However, total iron binding capacity (TIBC), a value that ordinarily correlates with transferrin concentration, was increased in BGN^{Tg} mice (Fig. 2d). Comparable effects were observed in male and female animals (data not shown), indicating that gender did not

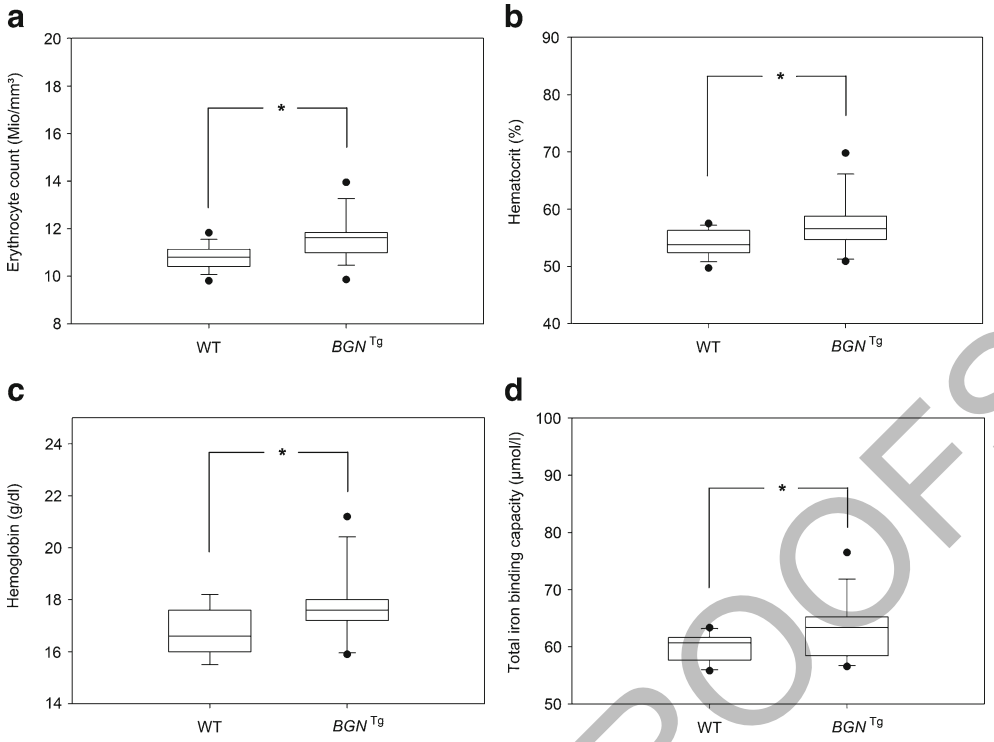

Fig. 2 Blood analysis of BGN^{Tg} mice reveals a hematological phenotype**.** Box Plot for (**a**) erythrocyte count, (**b**) hematocrit, (**c**) hemoglobin, and (**d**) total iron binding capacity (TIBC) in blood of WT and BGN^{Tg} mice as indicated; $n = 15$. Data represent means ± S.D.; *$P < 0.05$

alter the effect of biglycan overexpression. Taken together, these results show that overexpression of soluble biglycan induces a hematological phenotype characteristic of polycythemia.

Altered spleen morphology and elevated splenic iron deposition in BGN^{Tg} mice

In the course of their lifetime in circulation, erythrocytes undergo membrane changes which make them more susceptible to phagocytosis by macrophages, also referred to as eryptosis [34]. It is well established that polycythemia results in increased eryptosis marked by altered spleen morphology and enhanced splenic iron deposition [35, 36]. Thus, we determined whether stable overexpression of soluble biglycan would affect the overall splenic architecture and iron deposition. Histologic analysis using periodic acid-Schiff staining of the spleen revealed in BGN^{Tg} mice 2-fold enhancement of the red pulp (RP) area (Fig. 3a, b), the major site for senescent erythrocyte degradation [34]. In contrast, the white pulp (WP) and marginal zone architectures were comparable in BGN^{Tg} and WT mice (Fig. 3a). Furthermore, quantification of the RP/WP area showed an enhancement of this ratio in the spleen of BGN^{Tg} mice (WT 0.8 ± 0.5 vs. BGN^{Tg} 2.9 ± 1.2; $n = 6$, $P < 0.05$). Additionally, Perls' Prussian blue staining revealed an increased splenic deposition of the Fe^{3+}-storage complex hemosiderin in BGN^{Tg} mice (Fig. 3c, indicated by black arrows and quantified in Fig. 3d). These results demonstrate that the polycythemia in BGN^{Tg} mice coincides with increased RP area and iron deposition in the spleen, likely due to the augmented eryptosis.

Increased Epo expression and HIF-2α levels in liver and kidneys of BGN^{Tg} mice

A selective enhancement of erythrocytes in BGN^{Tg} mice implied that chronic overexpression of soluble biglycan may cause the development of secondary polycythemia. To test this hypothesis, we determined *Epo* expression in BGN^{Tg} mice. qRT-PCR analysis revealed a 1.6- and 2.3-fold induction of *Epo* mRNA expression in the liver and kidneys of BGN^{Tg} compared to WT mice (Fig. 4a). Furthermore, Epo protein levels as determined by a specific ELISA, were concurrently elevated in both parenchymal organs (Fig. 4b) and plasma (Fig. 4c) of BGN^{Tg} mice. Importantly, this enhancement (Fig. 4a-c) was associated with a 2-fold increase of HIF-2α protein levels in liver (WT 0.12 ± 0.03 vs. BGN^{Tg} 0.26 ± 0.04; $n = 3$; $P < 0.05$) and kidneys (WT 0.30 ± 0.02 vs. BGN^{Tg} 0.55 ± 0.10; $n = 3$; $P < 0.05$) of BGN^{Tg} mice (Fig. 4d). Higher HIF-2α protein abundance in liver and kidneys of mice overexpressing biglycan implicates involvement of this canonical transcription factor in biglycan-mediated effects on Epo synthesis. Interestingly, *HIF-2α* mRNA expression was not altered in liver (WT 1.00 ± 0.07 vs. BGN^{Tg} 0.95 ± 0.38, $n = 4$, n.s.) or kidneys (WT 1.05 ± 0.45 vs. BGN^{Tg} 0.94 ± 0.37; $n = 4$, n.s.) of BGN^{Tg} mice compared to WT mice. We conclude that

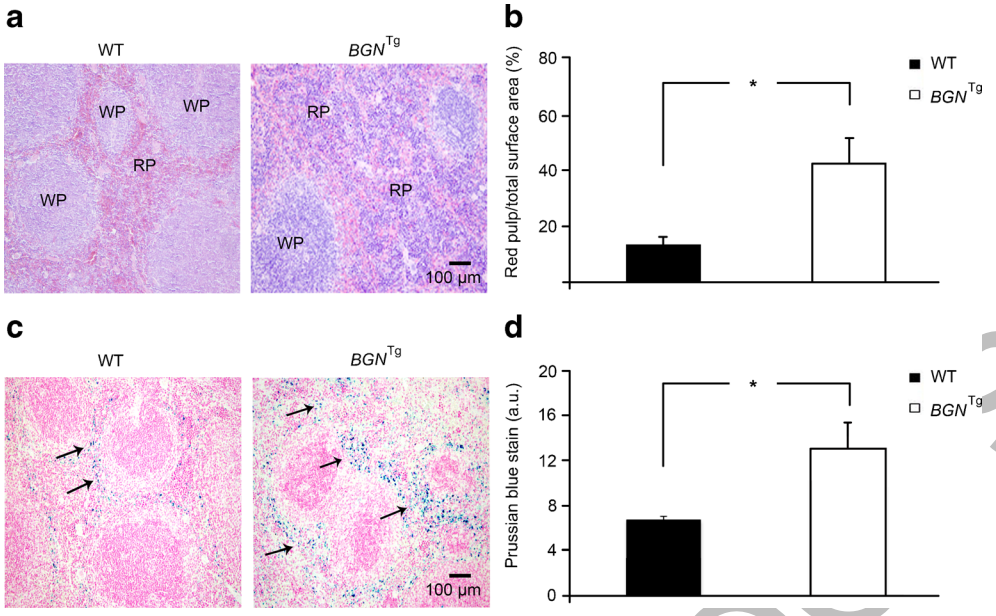

Fig. 3 BGN^{Tg} mice display altered spleen morphology and increased splenic iron deposition. (**a**) Representative histological images of PAS-stained WT and BGN^{Tg} spleen. White pulp (WP) is stained dark blue while red pulp (RP) locates between WP compartments. (**b**) Quantification of the percentage of red pulp area per total surface area in WT and BGN^{Tg} spleen; $n = 6$. Data represent means ± S.D.; $^*P < 0.05$. (**c**) Representative histological images of Perls' Prussian blue staining of WT and BGN^{Tg} spleen. The hemosiderin deposits are stained in blue (arrows). (**d**) Quantification of intensity of Perls' Prussian blue staining in arbitrary units (a.u.); $n = 6$. Data represent means ± S.D.; $^*P < 0.05$. (**a** and **c**) Scale bars represent 100 µm

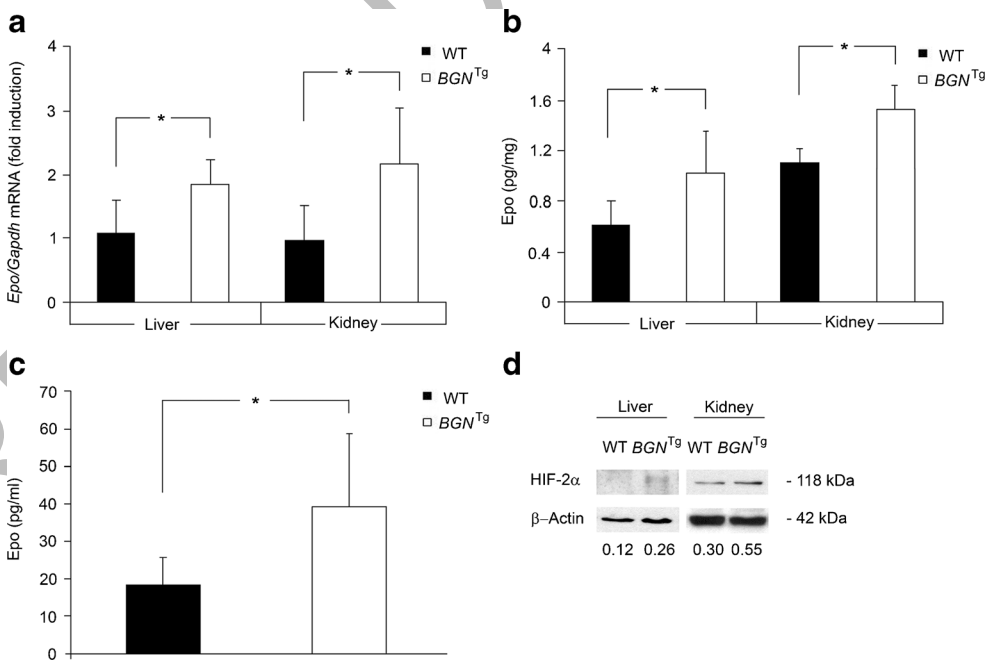

Fig. 4 Elevated Epo expression and HIF-2α level in the liver and kidneys of BGN^{Tg} mice. (**a**) Quantitative RT-PCR for *Epo* mRNA expression in liver and kidneys. Relative mRNA expression was normalized to *Gapdh* and given as fold induction compared to WT; $n = 8$. (**b**) ELISA for hepatic and renal Epo concentration in WT and BGN^{Tg} mice; $n = 8$. (**c**) ELISA for circulating Epo in plasma of WT and BGN^{Tg} mice; $n = 8$. (**d**) Representative immunoblot and quantification of HIF-2α in liver and kidneys of WT and BGN^{Tg} mice. Quantification of HIF-2α expression derives from three independent experiments quantified to β-Actin. (**a – c**) Data represent means ± S.D.; $^*P < 0.05$

chronic overexpression of soluble biglycan induces Epo synthesis and HIF-2α stabilization in the liver and kidneys, leading to secondary polycythemia.

TLR2 is required for biglycan-mediated Epo induction and polycythemia

Next, we searched for a mechanism of action of soluble biglycan-evoked Epo/HIF-2α levels. Accordingly, we transiently overexpressed soluble biglycan in WT mice as described previously [25–27]. We found that the plasma levels of Epo were significantly higher in mice injected with h*BGN* pLIVE for three days vis-à-vis mice injected with empty vectors (Fig. 5a). Concurrently, these mice displayed elevated HIF-2α protein level in liver (WT pLIVE 0.24 ± 0.01 vs. h*BGN* pLIVE 1.61 ± 0.14; $n = 3$; $P < 0.05$) and kidneys (WT pLIVE 0.14 ± 0.02 vs. h*BGN* pLIVE 0.66 ± 0.01; $n = 3$; $P < 0.05$) (Fig. 5b) as well as higher erythrocyte count (Fig. 5c). Collectively, our findings provide evidence for a direct involvement of soluble biglycan in the enhancement of Epo concentration, HIF-2α protein abundance and erythrocytes number.

Furthermore, we identified the receptor involved in this process. To this end, we transiently transfected WT, *Tlr2*$^{-/-}$,

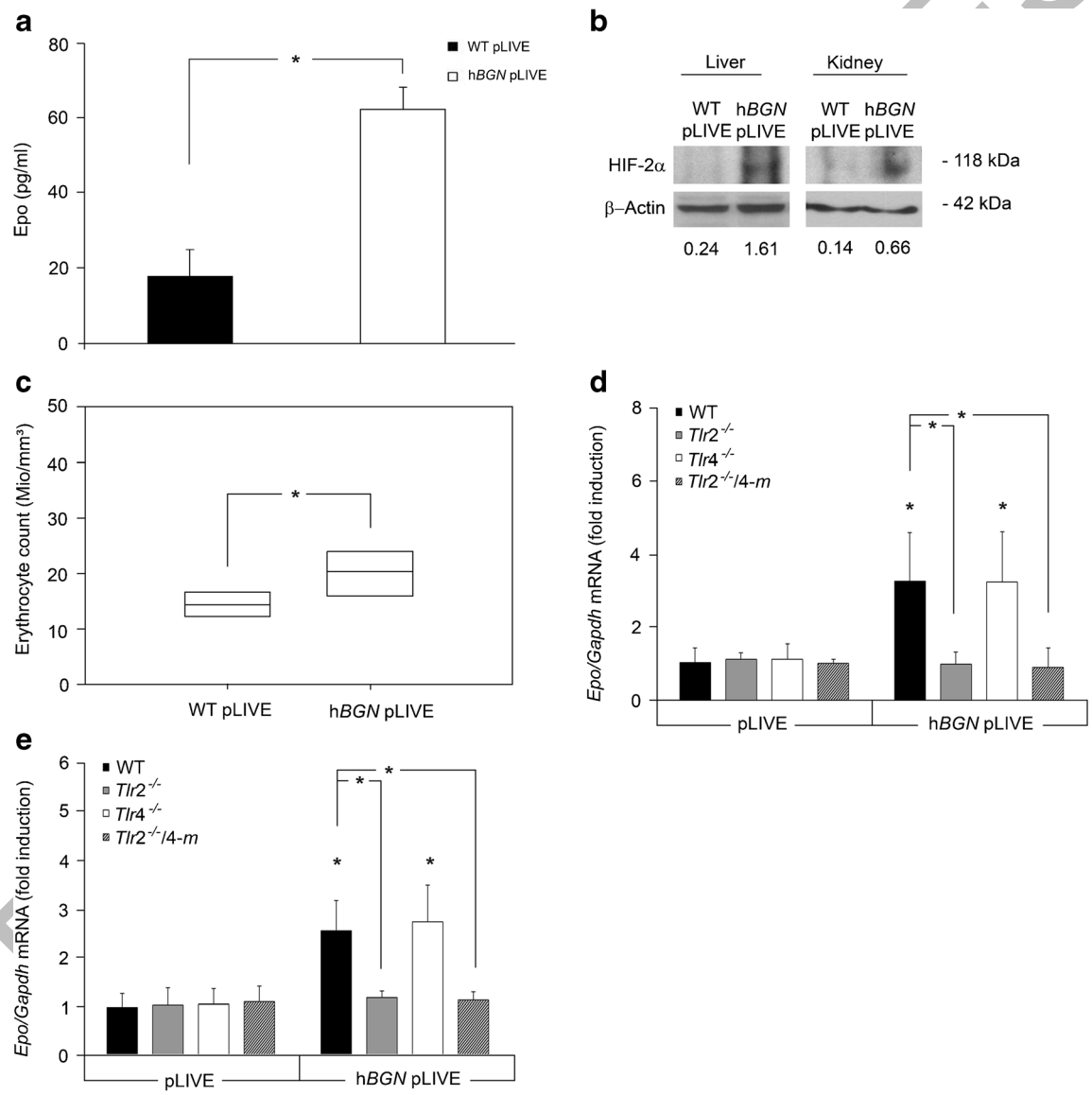

Fig. 5 Transient overexpression of biglycan induces Epo expression via TLR2 *in vivo* and evokes HIF-2α protein levels and erythrocytosis. (**a**) ELISA for Epo in plasma of control and biglycan-overexpressing mice; $n = 6$. (**b**) Representative immunoblot and quantification of HIF-2α protein levels in the liver and kidneys of WT mice 3 days after injection with either empty or h*BGN* containing pLIVE vector; $n = 3$. (**c**) Erythrocyte count in WT control and biglycan-overexpressing mice; $n = 6$. Quantitative RT-PCR for *Epo* mRNA expression in the (**d**) liver and (**e**) kidneys of WT and various mutant mice as indicated, 3 days after transfection with the pLIVE vector either empty (WT pLIVE) or carrying the human cDNA for biglycan (h*BGN* pLIVE). The mRNA data were normalized to *Gapdh*. Values represent means ± S.D.; *$P < 0.05$

Tlr4$^{-/-}$ and *Tlr2*$^{-/-}$*/4-m* mice (TLR-2-deficient mice carrying a functional mutation in the *Tlr4* gene) with h*BGN* pLIVE. In WT and *Tlr4*$^{-/-}$ mice, three days of biglycan transfection resulted in a marked overexpression of the *Epo* mRNA in the liver (Fig. 5d) and kidneys (Fig. 5e). In contrast, there was no difference in liver (Fig. 5d) and kidneys (Fig. 5e) of h*BGN* pLIVE transfected *Tlr2*$^{-/-}$ and *Tlr2*$^{-/-}$*/4-m* mice. Thus, we provide robust genetic evidence that soluble biglycan directly stimulates the expression of Epo in the liver and kidneys by selectively interacting with TLR2.

Discussion

In this study we describe the generation of a mouse model stably overexpressing soluble human biglycan (*BGN*^{Tg}), which displays increased Epo expression and HIF-2α stabilization in liver and kidneys, associated with the development of polycythemia. *BGN*^{Tg} mice overexpress human biglycan under an albumin promoter in the liver with subsequent secretion into the circulation and accumulation in various organs, here shown for the kidney. Although *BGN*^{Tg} mice appear healthy, blood analysis revealed a hematological phenotype characterized by increased erythrocyte number, hemoglobin concentration, hematocrit values and TIBC, consistent with a clinical picture of secondary polycythemia. Further investigations revealed elevated Epo concentrations in liver, kidneys and the circulation of *BGN*^{Tg} mice, coinciding with elevated erythrocyte counts, changes in the spleen structure and enhanced splenic iron deposition. In addition, *BGN*^{Tg} mice displayed higher hepatic and renal concentrations of HIF-2α, the key transcription factor known to regulate Epo expression [8, 9]. Moreover, transient overexpression of soluble biglycan for 3 days induced *Epo* mRNA expression in an exclusively TLR2-dependent manner in both liver and kidneys. We therefore hypothesize that this biological axis might be directly linked to higher HIF-2α levels in both parenchymal organs, liver and kidney, as well as circulating Epo concentrations and erythrocyte numbers. Our current working model is graphically depicted in Fig. 6.

Mice stably-transfected with human biglycan under the control of an albumin promoter displayed higher concentrations of biglycan in the circulation and organs that are equal to those found in experimental and human systemic disorders [25–27, 33]. Therefore, these transgenic mice provide a useful model to study consequences of a long-term exposure to soluble biglycan. In contrast, transient overexpression of soluble biglycan in mice deficient for various receptors or signaling molecules allows the *in vivo* identification of specific signaling pathways evoked by this proteoglycan, as shown here for TLR2. In our study we purposefully utilized the full-length human biglycan to allow a clear distinction between the endogenous murine and exogenous human product. We took

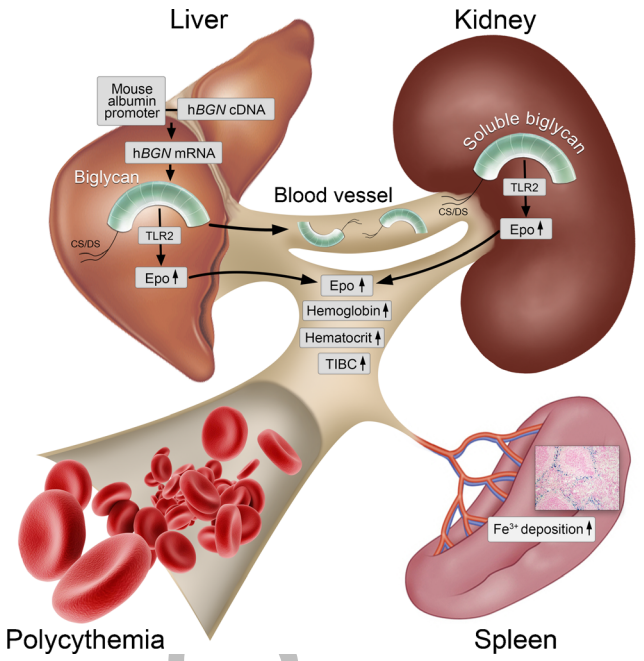

Fig. 6 Working model depicting the proposed mechanism of biglycan-mediated induction of Epo, HIF-2α and polycythemia. Human biglycan is overexpressed in the liver under an albumin promoter and secreted into the circulation resulting in accumulation in various organs (here shown for the kidney). By binding to TLR2, soluble biglycan triggers the expression of Epo in the liver and kidneys. Increased concentrations of circulating Epo in mice overexpressing soluble biglycan coincides with higher erythrocyte count, hemoglobin concentration, hematocrit values and total iron binding capacity (TIBC). Additionally, splenic red pulp area and iron deposition are elevated in *BGN*^{Tg} mice

advantage of a human-specific *Sac*I restriction site that allowed us to verify its transgenic expression in *BGN*^{Tg} livers. Lower intensity of murine biglycan expression band detected in *BGN*^{Tg} livers (Fig. 1e) was not due to suppressed endogenous biglycan, but was probably caused by reduced primer availability, as human (bp 573–1001) and murine biglycan (bp 585–1013) sequences show 90 % homology in their cDNA. By using primers distinguishing endogenous mouse from human biglycan, we detected equal expression of mouse biglycan in livers from WT and *BGN*^{Tg} mice.

BGN^{Tg} mice showed a clinical picture consistent with secondary erythrocytosis, which generally develops from excessive production of Epo secondary to systemic hypoxia, due to severe pulmonary disease, heart anomalies resulting in right-to-left shunting with blood bypassing the lungs, or high altitude syndrome. In such cases, the erythrocytosis is considered an appropriate compensatory response. If Epo production increases without systemic hypoxia, then the response is inappropriate. For example, there are several neuroendocrine tumors that have the ability to synthesize and release Epo into the blood stream and induce polycythemia. Although we have not measured the oxygen concentration in our mice, it is highly unlikely that our *BGN*^{Tg} mice are chronically hypoxic, given the fact that they appear normal, have normal weight and

reproduce as WT animals (see below). Histologic examination of the spleen showed an increase in the zone occupied by the red pulp suggesting extramedullary erythropoiesis. In addition, we observed a large increase in iron deposition in the red pulp, indicating increased uptake and catabolism of erythrocytes. During phagocytosis and degradation of erythrocytes, iron released from hemoglobin is bound by the iron storage complex hemosiderin [36]. These findings in the spleen are in full agreement with previously-published studies in mice affected by polycythemia [35, 37].

Both livers and kidneys of the BGN^{Tg} mice showed overexpression of Epo mRNA and protein, with consequently high levels of circulating Epo and secondary erythocytosis. Notably, we could validate these chronic changes using a transient transgenic mouse model [25–28], clearly indicating direct effects of soluble biglycan on Epo production and development of polycythemia. It was shown previously, that mice stably overexpressing human Epo develop secondary polycythemia [38, 39]. However, to our knowledge, this is the first report that a secreted matrix component is capable of triggering Epo expression and causing polycythemia.

It is well established that Epo expression is mainly regulated by HIF-2α [8]. Mice stably- and transiently-transfected with biglycan displayed higher HIF-2α protein abundance in liver and kidneys. As mRNA expression of *HIF-2α* was not induced in BGN^{Tg} mice we hypothesize that biglycan could cause HIF-2α stabilization [10, 13]. Stabilization of HIF-1α has been demonstrated to depend on the phosphorylation of Erk1/2 and p38 [40, 41]. Notably, biglycan regulates Epo expression by signaling via TLR2 and we have previously shown that this biglycan/TLR2 interactions activates both Erk1/2 and p38 pathways [22]. Thus, it is conceivable that a regulatory mechanism of biglycan-dependent HIF-2α stabilization might involve Erk1/2 and p38. Furthermore, ROS are potent stabilizers of HIF-2α protein [42]. Thus, biglycan by triggering ROS production [24] could stabilize HIF-2α. We have previously shown that decorin, a structurally-related proteoglycan [16], inhibits tumor angiogenesis by downregulating the mRNA and protein expression of constitutively-active HIF-1α in breast carcinoma cells [43]. Furthermore, treatment of retinal pigment epithelial cells with decorin effectively reduced the expression of HIF-1α under hypoxic conditions [44]. However in contrast to biglycan, decorin was involved in transcriptional regulation of HIF-1α and not in protein stabilization.

There is increasing evidence for oxygen-independent regulation of HIF-1α [15, 45]. In contrast, regulation of HIF-2α appears to be primarily controlled by the reduction in oxygen tension and by general hypoxic environmental conditions [46]. As BGN^{Tg} mice had normal growth, weight, lifespan and fertility and displayed no obvious clinical symptoms of chronic hypoxia, we postulate that biglycan-mediated regulation of HIF-2α and Epo occurs via a hypoxia-independent pathway.

Mechanistically, by transiently overexpressing biglycan in mice with genetic deletion of various TLRs, we demonstrated that biglycan-induced *Epo* mRNA expression in liver and kidneys is solely dependent on TLR2. The pro-inflammatory effects of biglycan are generally induced by a crosstalk between TLR2 and TLR4 [22, 25–27]. However, we have recently discovered an ability of biglycan to tightly regulate the inflammatory response via selective interaction with only one TLR [28]. Not much is known about the involvement of TLRs in Epo production. Up-to-date, only the involvement of TLR4 in erythropoiesis was proven in a model of *Salmonella* infection [47]. Thus biglycan signaling exclusively via TLR2 represents a new regulatory mechanism of Epo production and hence erythropoiesis.

The clinical relevance of our data is underlined by the finding that systemic biglycan overexpression effects red blood cell formation. As such, the use of biglycan as therapeutic protein, *e.g.* for amelioration of mild muscular dystrophy [48] should be approached cautiously. By contrast, patients with thalassemia suffering from anemia, iron overload and accelerated bone loss [49] might benefit from the numerous and newly identified functions of biglycan.

In summary, the novelty of our findings is three-fold: 1) This is the first report depicting a matrix component in its soluble form as a crucial trigger of Epo synthesis and inducer of secondary polycythemia. 2) We identify TLR2 as the key signaling receptor driving biglycan-dependent Epo synthesis. 3) We propose a new mechanism of posttranscriptional enhancement of HIF-2α protein by biglycan that is presumably an oxygen-independent HIF-2α stabilization. Although the clinical relevance of these findings is not yet known, we predict that enhanced levels of soluble biglycan might increase the clinical risk of thrombosis, cardiac infarction and stroke [1, 2].

Acknowledgments This study was supported by the German Research Council (SFB 815, project A5, SFB 1039, project B2, SFB 1177, project C2, and SCHA 1082/6-1), and LOEWE program Ub-Net (all to LS), the NIH grants CA39481 and NIH CA47282 (to RVI) and by the *01KX1012* Infrafrontier BMBF grants (to MHdA).

Compliance with ethical standards

Conflicts of interest The authors declare that they have no conflicts of interest.

Ethical approval This article does not contain any studies with human participants performed by any of the authors. All animal work was conducted in accordance with the German Animal Protection Law and was approved by the Ethics Review Committee for Laboratory Animals of the District Government of Darmstadt and Upper Bavaria, Germany.

Contributions All authors have approved the final article. HF conceived the project, performed experiments, analyzed data and wrote the manuscript. KM conceived and coordinated the project, analyzed data and wrote the manuscript. JZB generated the transgene mouse. LTH performed histology,

PG isolation and Western blots. BR carried out hematological and clinical-chemical tests and data interpretation. VGD, HF and MHdA participated in the coordination and conception of the hematological studies. RVI analyzed data and wrote the manuscript. LS conceived and coordinated the project, analyzed data and wrote the manuscript.

References

1. Hart R.G., Kanter M.C.: Hematologic disorders and ischemic stroke. A selective review. Stroke. **21**, 1111–1121 (1990)
2. Gordeuk V.R., Sergueeva A.I., Miasnikova G.Y., Okhotin D., Voloshin Y., Choyke P.L., Butman J.A., Jedlickova K., Prchal J.T., Polyakova L.A.: Congenital disorder of oxygen sensing: association of the homozygous Chuvash polycythemia VHL mutation with thrombosis and vascular abnormalities but not tumors. Blood. **103**, 3924–3932 (2004)
3. Berlin N.I.: Diagnosis and classification of the polycythemias. Semin. Hematol. **12**, 339–351 (1975)
4. Elliott S., Pham E., Macdougall I.C.: Erythropoietins: a common mechanism of action. Exp. Hematol. **36**, 1573–1584 (2008)
5. Zeisberg M., Kalluri R.: Physiology of the Renal Interstitium. Clin. J. Am. Soc. Nephrol. **10**, 1831–1840 (2015)
6. Lonnberg M., Garle M., Lonnberg L., Birgegard G.: Patients with anaemia can shift from kidney to liver production of erythropoietin as shown by glycoform analysis. J. Pharm. Biomed. Anal. **81-82**, 187–192 (2013)
7. Koury M.J., Bondurant M.C.: Erythropoietin retards DNA breakdown and prevents programmed death in erythroid progenitor cells. Science. **248**, 378–381 (1990)
8. Haase V.H.: Regulation of erythropoiesis by hypoxia-inducible factors. Blood Rev. **27**, 41–53 (2013)
9. Franke K., Gassmann M., Wielockx B.: Erythrocytosis: the HIF pathway in control. Blood. **122**, 1122–1128 (2013)
10. Lee F.S., Percy M.J.: The HIF pathway and erythrocytosis. Annu. Rev. Pathol. **6**, 165–192 (2010)
11. Percy M.J., Beer P.A., Campbell G., Dekker A.W., Green A.R., Oscier D., Rainey M.G., van Wijk R., Wood M., Lappin T.R., McMullin M.F., Lee F.S.: Novel exon 12 mutations in the HIF2A gene associated with erythrocytosis. Blood. **111**, 5400–5402 (2008)
12. Gale D.P., Harten S.K., Reid C.D., Tuddenham E.G., Maxwell P.H.: Autosomal dominant erythrocytosis and pulmonary arterial hypertension associated with an activating HIF2 alpha mutation. Blood. **112**, 919–921 (2008)
13. Jewell U.R., Kvietikova I., Scheid A., Bauer C., Wenger R.H., Gassmann M.: Induction of HIF-1alpha in response to hypoxia is instantaneous. FASEB J. **15**, 1312–1314 (2001)
14. Vriend J., Reiter R.J.: Melatonin and the von Hippel-Lindau/HIF-1 oxygen sensing mechanism: A review. Biochim. Biophys. Acta. **1865**, 176–183 (2016)
15. Agani F., Jiang B.H.: Oxygen-independent regulation of HIF-1: novel involvement of PI3K/AKT/mTOR pathway in cancer. Curr. Cancer Drug Targets. **13**, 245–251 (2013)
16. Iozzo R.V., Schaefer L.: Proteoglycan form and function: A comprehensive nomenclature of proteoglycans. Matrix Biol. **42**, 11–55 (2015)
17. Schaefer L.: Proteoglycans, key regulators of cell-matrix dynamics. Matrix Biol. **35**, 1–2 (2014)
18. Schaefer L.: Complexity of danger: the diverse nature of damage-associated molecular patterns. J. Biol. Chem. **289**, 35237–35245 (2014)
19. Hsieh L.T., Nastase M.V., Zeng-Brouwers J., Iozzo R.V., Schaefer L.: Soluble biglycan as a biomarker of inflammatory renal diseases. Int. J. Biochem. Cell Biol. **54**, 223–235 (2014)
20. Moreth K., Iozzo R.V., Schaefer L.: Small leucine-rich proteoglycans orchestrate receptor crosstalk during inflammation. Cell Cycle. **11**, 2084–2091 (2012)
21. Nastase M.V., Young M.F., Schaefer L.: Biglycan: a multivalent proteoglycan providing structure and signals. J. Histochem. Cytochem. **60**, 963–975 (2012)
22. Schaefer L., Babelova A., Kiss E., Hausser H.J., Baliova M., Krzyzankova M., Marsche G., Young M.F., Mihalik D., Gotte M., Malle E., Schaefer R.M., Grone H.J.: The matrix component biglycan is proinflammatory and signals through Toll-like receptors 4 and 2 in macrophages. J. Clin. Invest. **115**, 2223–2233 (2005)
23. Frey H., Schroeder N., Manon-Jensen T., Iozzo R.V., Schaefer L.: Biological interplay between proteoglycans and their innate immune receptors in inflammation. FEBS J. **280**, 2165–2179 (2013)
24. Babelova A., Moreth K., Tsalastra-Greul W., Zeng-Brouwers J., Eickelberg O., Young M.F., Bruckner P., Pfeilschifter J., Schaefer R.M., Grone H.J., Schaefer L.: Biglycan, a danger signal that activates the NLRP3 inflammasome via toll-like and P2X receptors. J. Biol. Chem. **284**, 24035–24048 (2009)
25. Moreth K., Brodbeck R., Babelova A., Gretz N., Spieker T., Zeng-Brouwers J., Pfeilschifter J., Young M.F., Schaefer R.M., Schaefer L.: The proteoglycan biglycan regulates expression of the B cell chemoattractant CXCL13 and aggravates murine lupus nephritis. J. Clin. Invest. **120**, 4251–4272 (2010)
26. Moreth K., Frey H., Hubo M., Zeng-Brouwers J., Nastase M.V., Hsieh L.T., Haceni R., Pfeilschifter J., Iozzo R.V., Schaefer L.: Biglycan-triggered TLR-2- and TLR-4-signaling exacerbates the pathophysiology of ischemic acute kidney injury. Matrix Biol. **35**, 143–151 (2014)
27. Zeng-Brouwers J., Beckmann J., Nastase M.V., Iozzo R.V., Schaefer L.: *De novo* expression of circulating biglycan evokes an innate inflammatory tissue response via MyD88/TRIF pathways. Matrix Biol. **35**, 132–142 (2013)
28. Hsieh L.T., Frey H., Nastase M.V., Tredup C., Hoffmann A., Poluzzi C., Zeng-Brouwers J., Manon-Jensen T., Schroder K., Brandes R.P., Iozzo R.V., Schaefer L.: Bimodal role of NADPH oxidases in the regulation of biglycan-triggered IL-1beta synthesis. Matrix Biol. **49**, 61–81 (2015)
29. Brattig N.W., Bazzocchi C., Kirschning C.J., Reiling N., Buttner D.W., Ceciliani F., Geisinger F., Hochrein H., Ernst M., Wagner H., Bandi C., Hoerauf A.: The major surface protein of Wolbachia endosymbionts in filarial nematodes elicits immune responses through TLR2 and TLR4. J. Immunol. **173**, 437–445 (2004)
30. Poltorak A., He X., Smirnova I., Liu M.Y., Van Huffel C., Du X., Birdwell D., Alejos E., Silva M., Galanos C., Freudenberg M., Ricciardi-Castagnoli P., Layton B., Beutler B.: Defective LPS signaling in C3H/HeJ and C57BL/10ScCr mice: mutations in Tlr4 gene. Science. **282**, 2085–2088 (1998)
31. Rathkolb B., Fuchs H., Gailus-Durner V., Aigner B., Wolf E., Hrabe de Angelis M.: Blood Collection from Mice and Hematological Analyses on Mouse Blood. Curr. Protoc. Mouse Biol. **3**, 101–119 (2013)
32. Rathkolb B., Hans W., Prehn C., Fuchs H., Gailus-Durner V., Aigner B., Adamski J., Wolf E., Hrabe de Angelis M.: Clinical Chemistry and Other Laboratory Tests on Mouse Plasma or Serum. Curr. Protoc. Mouse Biol. **3**, 69–100 (2013)
33. Schaefer L., Raslik I., Grone H.J., Schonherr E., Macakova K., Ugorcakova J., Budny S., Schaefer R.M., Kresse H.: Small proteoglycans in human diabetic nephropathy: discrepancy between glomerular expression and protein accumulation of decorin, biglycan, lumican, and fibromodulin. FASEB J. **15**, 559–561 (2001)
34. Lang F., Lang E., Foller M.: Physiology and pathophysiology of eryptosis. Transfus. Med. Hemother. **39**, 308–314 (2012)
35. Kaufmann K.B., Grunder A., Hadlich T., Wehrle J., Gothwal M., Bogeska R., Seeger T.S., Kayser S., Pham K.B., Jutzi J.S., Ganzenmuller L., Steinemann D., Schlegelberger B., Wagner

J.M., Jung M., Will B., Steidl U., Aumann K., Werner M., Gunther T., Schule R., Rambaldi A., Pahl H.L.: A novel murine model of myeloproliferative disorders generated by overexpression of the transcription factor NF-E2. J. Exp. Med. **209**, 35–50 (2012)
36. Cesta M.F.: Normal structure, function, and histology of the spleen. Toxicol. Pathol. **34**, 455–465 (2006)
37. Guihard S., Clay D., Cocault L., Saulnier N., Opolon P., Souyri M., Pages G., Pouyssegur J., Porteu F., Gaudry M.: The MAPK ERK1 is a negative regulator of the adult steady-state splenic erythropoiesis. Blood. **115**, 3686–3694 (2010)
38. Wagner K.F., Katschinski D.M., Hasegawa J., Schumacher D., Meller B., Gembruch U., Schramm U., Jelkmann W., Gassmann M., Fandrey J.: Chronic inborn erythrocytosis leads to cardiac dysfunction and premature death in mice overexpressing erythropoietin. Blood. **97**, 536–542 (2001)
39. Vogel J., Kiessling I., Heinicke K., Stallmach T., Ossent P., Vogel O., Aulmann M., Frietsch T., Schmid-Schonbein H., Kuschinsky W., Gassmann M.: Transgenic mice overexpressing erythropoietin adapt to excessive erythrocytosis by regulating blood viscosity. Blood. **102**, 2278–2284 (2003)
40. Michiels C., Minet E., Michel G., Mottet D., Piret J.P., Raes M.: HIF-1 and AP-1 cooperate to increase gene expression in hypoxia: role of MAP kinases. IUBMB Life. **52**, 49–53 (2001)
41. Richard D.E., Berra E., Gothie E., Roux D., Pouyssegur J.: p42/p44 mitogen-activated protein kinases phosphorylate hypoxia-inducible factor 1alpha (HIF-1alpha) and enhance the transcriptional activity of HIF-1. J. Biol. Chem. **274**, 32631–32637 (1999)
42. Guzy R.D., Hoyos B., Robin E., Chen H., Liu L., Mansfield K.D., Simon M.C., Hammerling U., Schumacker P.T.: Mitochondrial complex III is required for hypoxia-induced ROS production and cellular oxygen sensing. Cell Metab. **1**, 401–408 (2005)
43. Neill T., Painter H., Buraschi S., Owens R.T., Lisanti M.P., Schaefer L., Iozzo R.V.: Decorin antagonizes the angiogenic network: concurrent inhibition of Met, hypoxia inducible factor 1alpha, vascular endothelial growth factor A, and induction of thrombospondin-1 and TIMP3. J. Biol. Chem. **287**, 5492–5506 (2011)
44. Du S., Wang S., Wu Q., Hu J., Li T.: Decorin inhibits angiogenic potential of choroid-retinal endothelial cells by downregulating hypoxia-induced Met, Rac1, HIF-1alpha and VEGF expression in cocultured retinal pigment epithelial cells. Exp. Eye Res. **116**, 151–160 (2013)
45. Loboda A., Jozkowicz A., Dulak J.: HIF-1 and HIF-2 transcription factors–similar but not identical. Mol. Cells. **29**, 435–442 (2010)
46. Rankin E.B., Giaccia A.J.: Hypoxic control of metastasis. Science. **352**, 175–180 (2016)
47. Jackson A., Nanton M.R., O'Donnell H., Akue A.D., McSorley S.J.: Innate immune activation during Salmonella infection initiates extramedullary erythropoiesis and splenomegaly. J. Immunol. **185**, 6198–6204 (2010)
48. Casar J.C., McKechnie B.A., Fallon J.R., Young M.F., Brandan E.: Transient up-regulation of biglycan during skeletal muscle regeneration: delayed fiber growth along with decorin increase in biglycan-deficient mice. Dev. Biol. **268**, 358–371 (2004)
49. Wong, P., Fuller, P.J., Gillespie, M.T., Milat, F.: Bone Disease in Thalassemia: A Molecular and Clinical Overview. Endocr. Rev.: p. er20151105 (2016)